

Layer-by-layer assembly of chitosan and platelet monoclonal antibody to improve biocompatibility and release character of PLLA coated stent

L. L. Luo,¹ G. X. Wang,¹ Y. L. Li,¹ T. Y. Yin,¹ T. Jiang,¹ C. G. Ruan²

¹Key Laboratory of Biorheological Science and Technology (Chongqing University), Ministry of Education, Chongqing Engineering Laboratory in Vascular Implants, Bioengineering College of Chongqing University, Chongqing 400044, China

²Jiangshu Institute of Hematology, The First Affiliated Hospital of Suzhou University, Suzhou, China

Received 24 September 2010; revised 19 November 2010; accepted 4 January 2011

Published online 11 April 2011 in Wiley Online Library (wileyonlinelibrary.com). DOI: 10.1002/jbm.a.33066

Abstract: The aim of this study is to construct a biocompatible coating of a drug-eluting stent through the incorporation of chitosan with monoclonal antibody (mAb) to a platelet glycoprotein (GP) IIIa receptor, by electrostatic layer-by-layer (LBL) adsorption of oppositely charged polyelectrolytes and proteins. The platelet maximum aggregation rate and aggregation inhibition rate tests confirm the bioactivity of mAb in different pH assembly environments. The fluorescence spectra test and confocal laser scanning microscopy observation were used to monitor the LBL assembly process of the mAb/chitosan multilayer on the surface of the aminolyzed Poly-L-lactic acid (PLLA) membrane, when using Rhodamine B isothiocyanate-labeled mAb and Fluorescein isothiocyanate-labeled chitosan. The *in vitro* platelet adhesion experiment demonstrated the amicable blood compatibility of the mAb/chitosan multilayer. The endothelial cell adhesion and migration test revealed that the multi-

layer could improve the cytocompatibility of the PLLA matrix in terms of cell attachment, proliferation, and migration. An *in vitro* perfusion circuit was designed to evaluate the release rates measured by a radioisotope technique with ¹²⁵I-labeled GP IIIa mAb. The different eluting curves of the mAb/chitosan-assembled stent and mAb physically absorbed stent showed the improvement of mAb's release character when using LBL self-assembly technology. Our method to prepare a biocompatible stent surface with mAb/chitosan multilayers has proved to be favorable and effective *in vitro*, thus justifying further evaluation to improve the biocompatibility in an animal model test. © 2011 Wiley Periodicals, Inc. *J Biomed Mater Res Part A*: 97A: 423–432, 2011.

Key Words: drug eluting stent, L-poly(lactic acid) coating, monoclonal antibody, chitosan, layer-by-layer self-assembly

INTRODUCTION

Percutaneous transluminal coronary angioplasty (PTCA) is widely used for the treatment of occlusive blood vessel diseases.¹ During the last two decades, intravascular coronary stenting has been widely used, which has improved the safety of the PTCA procedures and has been shown to reduce restenosis.^{2–4} However, the initial goal of the stent to inhibit restenosis is not satisfactorily achieved for the in-stent restenosis (ISR). Several results^{5–7} have shown that ISR occurs in about 20% to 30% after stenting procedures, although the rate of restenosis is 10% lower compared to stent with PTCA procedures. Further to many “trials-and-errors,” the drug-eluting stent (DES) has emerged as an undisputed solution to prevent ISR.^{8–10} However, the data of recent research^{11–13} reveal that in-stent thrombosis, especially late angiographic stent thrombosis (LAST), is the most serious complication of DES, because most of the affected patients die or suffer a myocardial infarction, in spite of its low incidence. The DES stents are usually coated with a bioresorbable polymer matrix, capable of releasing single or multiple bioactive agents into

the bloodstream and surrounding tissues. Early studies on stents coated with biodegradable polymers were disappointing and indicated that the polymers triggered long-term inflammation.¹⁴ The delay of endothelialization and formation of thrombosis may be ascribed to the polymer coating on the stent surface.¹⁵ To avoid the undesirable effects of currently applied (durable) polymers, biocompatible and bioabsorbable polymers as well as DES delivery systems, which minimize polymer burden, have been produced and tested.¹⁶ In addition to the negative influence of polymers, the drug loaded in the DES (e.g., Rapamycin of CypherTM and Paclitaxel of TaxusTM) is supposed to be another important trigger for LAST, because it may also delay the endothelialization and healing on the stent surface.¹⁷ Therefore, the ideal agents for stent coatings should inhibit thrombus formation, inflammatory reaction, and cellular proliferation, while supporting re-endothelialization.

The goal of the new DES technology should be to balance the benefits of restenosis prevention against the risks of delayed healing and late stent thrombosis.¹⁸ The

Correspondence to: G. X. Wang; e-mail: wanggx@cqu.edu.cn

Contract grant sponsor: Ministry of Science and Technology of China (Internationally Scientific and Technological Cooperation); contract grant number: 2004DFA06400

Contract grant sponsor: National Natural Science Foundation of China; contract grant number: 30970721

TABLE I. The Ratio of Different pH Buffers (v/v)

	pH4	pH5	pH6	pH7	pH8
Sodium hydrogen phosphate solution (0.2M)	2.055	3.855	5.15	6.315	8.235
Sodium citrate solution (0.1M)	7.945	6.145	4.85	3.685	1.765

development of a biocompatible coating strategy of the stent has become the competitive hot-spot in the research of a new generation coronary stent system. The usual method was to modify the stent coating with hydrophilic agents, such as, heparin,^{15,19} phosphorylcholine,²⁰ fibrin,²¹ poly(ethylene oxide),²² and platelet glycoprotein (GP) IIb/IIIa receptor antibody.^{23,24} All the stents were validated, but the results of re-endothelialization in stent microenvironment were ambiguous. In recent times, it has been also reported that coronary stents were coated with anti-CD34 antibodies, which captured a patient's endothelial progenitor cells to accelerate the natural healing process.²⁵ The applied prospect of this stent is very attractive, but the preprocess and postprocess of stent deployment included production, sterilization, and a biological response.

The stent coatings need to satisfy many of the physical, biological, and regulatory criteria before they can be deemed suitable, therefore, the most important factor is to choose a suitable and convenient method for coating the stent. The coating solution is often applied to the stent in the traditional manner in which liquid solution is applied, such as, dipping, spraying, or brushing.²⁶⁻²⁸ Of late, the layer-by-layer (LBL) assembly technology, a technique in which nanoscale layers of polyanions and polycations are dipped onto a charged surface from aqueous baths, constitutes a powerful tool, with applications ranging from electrochemical thin films to biocatalysis.²⁹ The monoclonal platelet GP IIIa receptor antibody was used in our previous study,^{30,31} to construct an mAb eluting stent. The stent system may lead to a significant reduction in stent thrombosis because the antibody can block the GP IIb/IIIa receptor, to prevent platelet aggregation.³² However, because of the hydrophilic character of the protein and the application of the passive absorption method, the release characteristics of the SZ-21 eluting stent *in vitro* shows similar properties, with standard characteristics of the protein absorbed, when released from the surface of the solid matrix.³¹ The LBL self-assembly technology has the advantage of utilizing mild aqueous baths that have the potential to preserve fragile protein activity in comparison to the harsh organic solvents typically employed to fabricate protein delivery devices.³³

Our hypothesis results from the fact that electrical properties of the monoclonal platelet GP IIIa receptor antibody, as one type of protein, can be controlled in different pH solutions, based on its isoelectric point ($PI_{mAb} = 6.9$). The other material, chitosan, is now widely studied and used as a matrix for tissue engineering and drug release, because of its good biocompatibility and biodegradability. It has been reported that chitosan plays a critical role in cell attachment and growth.^{34,35} It also has been used to construct an ultra-

thin coating layer on the stent surface as one natural cationic polyelectrolyte.^{15,36,37} Therefore, in this study, we have tried to construct one biocompatible stent surface using LBL self-assembly technology, to assemble the mAb/chitosan multilayer, which could improve the mAb release character, and maintain the antithrombosis performance of the stent, and at the same time, promote the healing of the endothelium on the stent surface.

MATERIALS AND METHODS

Evaluation of mAb's antiplatelet aggregation in different pH buffers

The buffer with different hydrogen ion concentrations was prepared by mixing different quantities of 0.2M sodium hydrogen phosphate solution and 0.1M sodium citrate solution (purchased from the Chuandong Chemical Co., Chongqing, China), as shown in Table I. The freeze-dried powder of SZ-21, one type of platelet GP IIb/IIIa mAb (supplied by the Jiangshu Institute of Hematology, Suzhou, China), was prepared at concentration of 1 mg/mL in the different pH buffers. Arterial blood was collected using cardiac puncture surgery, using New Zealand White rabbits (purchased from The Animal Research Center of Xinqiao Hospital, Chongqing, China). Sodium citrate of 3.8% was added to the blood as an anticoagulant, with the ratio of blood/anticoagulant being 9:1. First, the blood was centrifuged at 800 rpm for 10 min using the Eppendorf 5417R refrigerated microcentrifuge (Eppendorf China, Shanghai, China) to obtain platelet rich plasma (PRP). Then the blood was centrifuged at 3000 rpm for 15 min to obtain platelet poor plasma (PPP). The PA100 platelet aggregation instrument (Tianhai Medical Instrument Co., Chongqing, China), based on Born's turbidimetry³⁸ method, was used to monitor the influence of SZ-21 on platelet aggregation in different pH buffers, by automatically recording the platelet aggregation curve. The inducer of platelet aggregation was ADP, with a final concentration of 2 μ mol/L. A total of 5 μ L SZ-21 solution in different pH buffers and 20 μ L ADP were added in 200 μ L PRP, with 5 μ L of a corresponding pH buffer added in 200 μ L PRP as the control, to obtain the influence of SZ-21 on the platelet maximum aggregation rate (MAR). The aggregation inhibition rate (AIR) could be calculated with the formula (1):

$$AIR(\%) = \frac{MAR_{control} - MAR_{mAb}}{MAR_{control}} \times 100\% \quad (1)$$

Preparation and characterization of mAb/chitosan multilayer on PLLA membrane

Our purpose was to assemble the SZ-21/chitosan multilayer on the surface of the PLLA coated stent, hence, the PLLA

membrane (1 cm × 1 cm, 100 μm thickness, purchased from Jinan Daigang Co., Shangdong, China) was used to facilitate the characterization of the LBL process. The PLLA membrane was first aminolyzed using the method as reported.³⁹ The SZ-21 and chitosan (purchased from Sigma, St. Louis, MO) were selected as the building blocks to modify the aminolyzed PLLA membranes, using the LBL assembly technique. The aminolyzed PLLA membranes were treated in 0.01M HCl solution for 30 min, at room temperature, and washed with a large amount of water to ensure the charged state of the substrata. After washing with a large amount of water, the membranes were placed for 20 min into the 2 mg/mL SZ-21 solution prepared with pH8 buffer and rinsed with pure water. The SZ-21 modified membranes were subsequently immersed in the chitosan solution made with 0.2 wt % acetic acid and 0.1 wt % chitosan, for 20 min, followed by the same rinsing procedure. The process was repeated until the desired number of layers had been deposited. Finally, the samples were dried at 30°C under reduced pressure for 48 h to obtain the SZ-21/chitosan multilayer on the surface of the PLLA membrane.

To monitor the assembly process of the two kinds of materials on the aminolyzed PLLA surface, the SZ-21 and chitosan were respectively substituted with Rhodamine B isothiocyanate (RBITC)-labeled SZ-21 and Fluorescein isothiocyanate (FITC)-labeled chitosan (labeled by Biosynthesis Biotechnology Co., Beijing, China) to form the (RBITC-labeled SZ-21/CH)_n and (SZ-21/FITC-labeled CH)_n multilayer, with layers from one to 10. For preventing fluorescent quenching, the entire procedure was processed in a dark environment. Fluorescence spectra tests were performed on a Shimadzu RF5301PC fluorescence spectrophotometer at room temperature. The (RBITC-labeled SZ-21/FITC-labeled CH)_n multilayer was also prepared, to be scanned with 300 nm scan space by the z-scan mode of Leica TCSNT laser scanning confocal microscope(LSCM), for verifying the distribution of the two kinds of materials in the self-assembly multilayer.

***In vitro* hemocompatibility evaluation**

The blood was collected and handled using the method mentioned earlier, to obtain PRP and PPP. To evaluate the platelet adhesion character, the SZ-21/chitosan assembled membranes, with 10 bilayers, were immersed into the PRP and incubated at 37°C for 3 h, followed by rinsing with 0.9% NaCl solution, to remove the weakly adherent platelets. The adhered platelets were fixed in a 2.5% glutaraldehyde solution, and then dehydrated and dried at the critical point. The samples were coated with a gold layer of 10–20 nm thickness and examined by scanning electron microscopy (SEM, Vega-LMH, Tescan, Czech). The anticoagulant property of the SZ-21/chitosan assembled membranes were determined by activated partial thrombin time (APTT) and prothrombin time (PT) assays.⁴⁰ SZ-21/chitosan assembled membranes were placed carefully into tubes and incubated in 0.5 mL of PPP at 37°C for 30 min. For APTT, 50 μL residual PPP was put into a special test tube and then the 50 μL

APTT reagent (Sichuan Maker Science Technology Co., China) was added into the above-mentioned tube. Another 0.025M CaCl₂ solution (50 μL) was then added after 3 min of incubation at 37°C. For PT, 50 μL residual PPP was mixed with 100 μL PT reagent (Sichuan Maker Science Technology Co., China). The clotting time of the solution was measured by a coagulometer (CA-50, Sysmex, Japan). In evaluation of the platelet adhesion, APTT and PT assays and aminolyzed PLLA membranes, without assembled process, were used as the positive control and PLLA membranes without aminolyzed process were used as the negative control.

Adhesion and migration of endothelial cells

The endothelial hybrid cell line Eahy926 (from Third Military Medical University, Chongqing, China) was adopted to observe cell adhesion and migration on the assembled membranes. The cells were cultured in Dulbecco's modified eagle medium supplemented with 10% fetal calf serum (FCS), and maintained in 5% CO₂ atmosphere at 37°C and 96% humidity. Cell passages were carried out once or twice a week at a ratio of 1:3. Upon reaching cell confluence of 70%–80%, the cells were washed with phosphate-buffered saline (PBS) and trypsinized for 2 min at 37°C. Trypsin was neutralized by adding a culture medium containing 10% FCS. Sterilized samples of the assembled and nonassembled membranes were placed in the wells of a six-well culture plate. The cells were seeded onto these samples surfaces at 2.0×10^4 in the culture medium and grew for 48 h, respectively. The samples were subsequently rinsed with 0.9% NaCl solution to remove the weakly adherent endothelial cells. The adhered cells were fixed in a 2.5% glutaraldehyde solution at room temperature for 2 h, and then dehydrated and critically point-dried. The specimens were then coated with a gold layer of 10–20 nm thickness and were examined by SEM to investigate the morphology of the adherent endothelial cells. To evaluate the cell migration on the membranes, a sterile scraper was used to carefully scrape off the cells along the midline of the membranes, while being viewed under an Olympus BX51 inverted microscope, until all the samples were fully covered with cells. Then the remaining cells on the samples were incubated at 37°C. Time-lapse phase contrast images were captured every 30 min using the microscope combined with a Metamorph program. Cells were continuously observed and counted for 72 h.

Evaluation of mAb's release from the multilayer

Stainless steel coronary stents, 316 L, (bare metal stents) 17 mm long and 1.4 mm in diameter (MeiZhongShuangHe Medical Device, Beijing, China) were dipped in K₂Cr₂O₇/H₂SO₄ solution (1/9 v/v) for 10 min at 30°C, then washed thrice with sterile double distilled water. After being dried at 70°C in a vacuum oven, the stent was coated with PLLA (purchased from Sigma, St. Louis, MO) using the ultrasonic atomization spraying system.⁴¹ The PLLA coated stent was aminolyzed followed by the assembly with a SZ-21/chitosan multilayer, using the methods mentioned earlier. To facilitate the evaluation of mAb's release character, the SZ-21 was

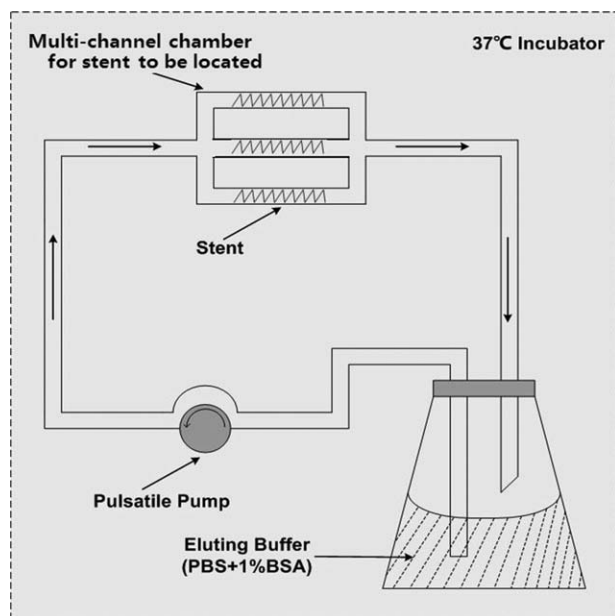


FIGURE 1. Schematic diagram of the experimental perfusion system for elution of mAb from stent wires *in vitro*. The stent wires are parallelly located in the multi-channel chamber, and perfused with 1% BSA in PBS for different duration and pulsatile flow produced by pulsatile pump. The entire system is placed in the incubator with 37°C temperature.

first radio-labeled with ^{125}I , using the standard Iodogen method. Five microliters of labeled mAb SZ-21 was added into the 2 mg/mL SZ-21 solution during the assembly process, thus the amount of SZ-21 could be represented by the radioactivity of the stent, counted with a γ -counter (DFM-96, Zhongchen, Hefei, China). The perfusion system of the flow chamber, as shown in Figure 1, was also developed to evaluate the release characteristics of the mAb SZ-21 from the SZ-21/chitosan multilayer. The system was located in a 37°C incubator when perfusion with 150 mL flow buffer was prepared with 1% Bovine Serum Albumin (Sigma-Aldrich, St. Louis, MO, USA) added to PBS (0.01M/L,

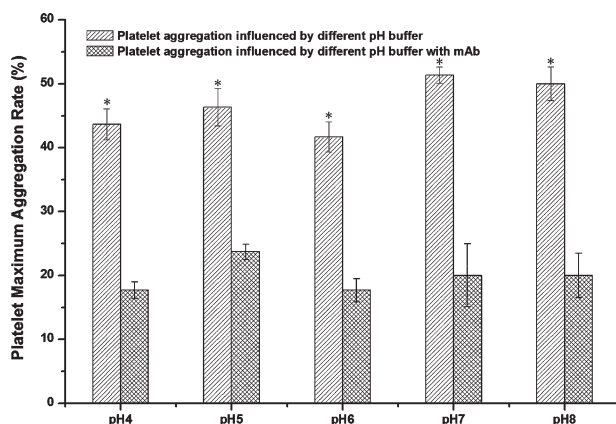


FIGURE 2. Results of platelet MAR tested by PA100 platelet aggregation instrument show that the platelet aggregation is inhibited by SZ-21 mAb in each pH buffer group (* $p < 0.05$, $n = 6$).

pH 7.4), to satisfy the expected conditions. Before being located in the chamber, the quantity of SZ-21 on the stents with different SZ-21/chitosan layers was calculated by counting its radioactivity. At every scheduled time point ranging from 30 min to 312 h, the residual amount of SZ-21 was determined through the above-mentioned radioactivity counting method for drawing the *in vitro* release curve of the SZ-21/chitosan modified stent. For comparison, the PLLA stent without aminolysis and assembly process was also directly immersed into the SZ-21 solution of the same concentration, to prepare the physically adsorbed stent for distinguishing their release character from the assembled ones.

Statistical analysis

Significance of variability among the means of experimental groups was determined by one-way or two-way analysis of variance using SPSS for Windows V15.0 software. Differences among experimental groups were considered to be statistically significant when $p < 0.05$. Unless indicated, values are given as mean \pm SD.

RESULTS

The influence of pH value to mAb's activity

Figure 2 shows the platelet MAR in different pH buffers with mAb, which is an important bioactive agent to be assembled in this study. It can be seen that when adding the mAb in the five groups with different pH values, the aggregation of the platelet is inhibited to a large extent. The AIR results have been used to evaluate the influence of pH on the mAb activity, as shown in Figure 3. Through comparison of the AIR of mAb in five pH buffers, it has been found that the antiplatelet of mAb is not influenced by the pH buffer ($p > 0.05$, $n = 6$), which may be an important factor to use mAb as one composition of the self-assemble multilayer.

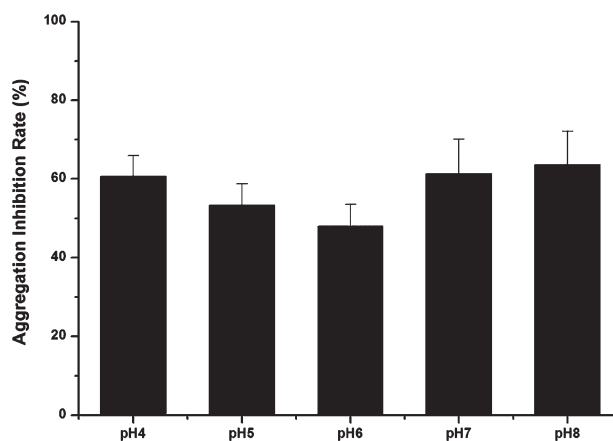


FIGURE 3. Results of aggregation rate calculated with formula one show that the influence of pH is not significant ($p > 0.05$, $n = 6$), which prove that the mAb can play the normal biological function when added in different pH buffer.

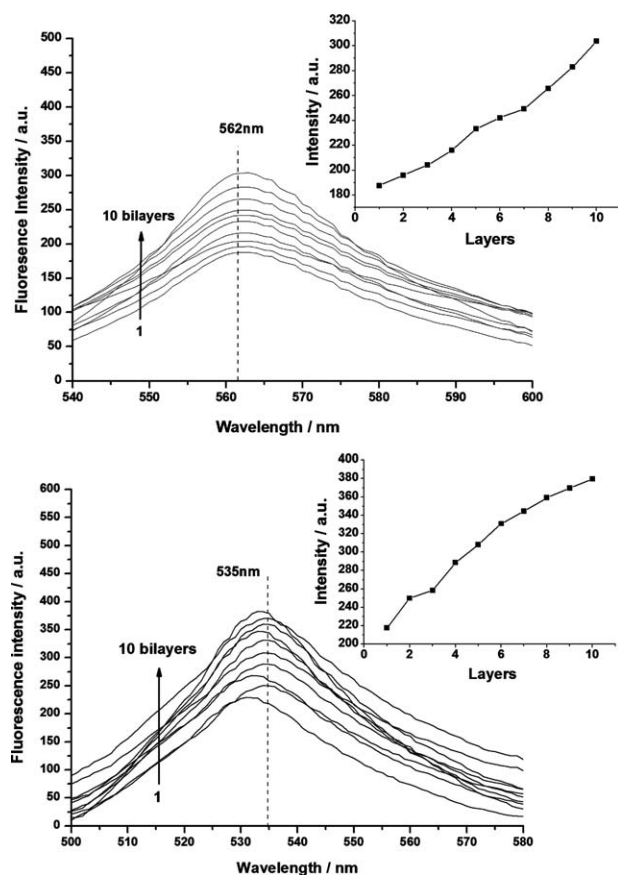


FIGURE 4. Fluorescence curve of RBITC-labelled SZ-21 (the upper) and FITC-labelled chitosan (the lower) show that the two compositions can be assembled with layer by layer technology. The relative curve of intensity and layers of SZ-21 in 562 nm and chitosan in 535 nm is respectively shown in the upper right and lower right of the figure, which clearly display the basic linear growth trend of SZ-21 and chitosan.

Evaluation the assembly process of the multilayer

For the sake of convenient monitoring of the assembly process, fluorescence spectroscopy was adopted to monitor the layer growth of the SZ-21/chitosan multilayer by respectively substituting the normal SZ-21 with RBITC-labeled SZ-21 and normal chitosan with FITC-labeled chitosan. The spectra in the two figures exhibited the maximum emission at ~ 560 nm arising from the rhodamine group (excitation wavelength was 520 nm) and at ~ 535 nm, arising from the FITC group (excitation wavelength was 490 nm), respectively, as shown in Figure 4. As could be seen from the two profiles, the two compositions in the composite multilayer, represented by the maximum emission, increased with an increase in layer number, which had a basic trend of linear relationship between the layers and the fluorescence intensity. Therefore, it could be deduced that the increase in the thickness of the assembled material had a certain vertical uniformity. The mapping relation curve between the assembled layers and the maximum emission intensity at 562 nm (RBITC-labeled SZ-21) or 535 nm (FITC-labeled chitosan) could clearly monitor the self-assembly process. For SZ-21, the increased trend was more linear from the first to

the fourth layers and the seventh to the 10th layers, but the linear increase showed a slight change from the fifth to the seventh layers. The reason for this phenomenon perhaps resulted from the change of the net charge on the antibody surface, on account of the interpenetration between the assembled layers. For chitosan, the initial assembly layers were slightly different from the others, which could be related to the defects on the substrate surface. This was often observed in an LBL assembly of polyelectrolytes on the planar substrata.⁴²

For clearly observing the distribution of the two compositions in the multilayer along the vertical dimension, the two fluorescent-labeled materials were used for assembly and the different color monolayers were then scanned with LSM at the z-scan mode. In the 3 μm range of scan depth, there were four major distributions of SZ-21 (red) and chitosan (green), as shown in the Figure 5. In their respective layer, the SZ-21 [Fig. 5(A)] and chitosan [Fig. 5(C)] were distributed more evenly, but there was the phenomenon of interpenetration between the layers [Fig. 5(B,D)]. Figure 5(B) reflected the transition from the SZ-21 monolayer to the chitosan monolayer, while the opposite state is presented in Figure 5(D). The existence of a single color fluorescent layer, as shown in Figure 5(A,C), revealed that one material penetrated into a part of the other monolayer, rather than through the entire layer of another material.

In vitro hemocompatibility of the assembled multilayers

The morphology of the adhered platelets on the negative, positive and SZ-21/chitosan assembled membranes, after 3 h of incubation in PRP, is displayed in Figure 6, which was the result of the SEM field chosen at random. The platelets on the assembled membrane were isolated [shown as Fig. 6(C)]. There was no sign of accumulation and almost no pseudopodium could be observed. In contrast, there was slight platelet accumulation, and the pseudopodium of platelets was visible on the surface of aminolyzed PLLA membranes [shown as Fig. 6(B)], and more severe accumulation and pseudopodium of platelets presented on the surface of the PLLA membranes [shown as Fig. 6(A)]. The aminolyzed process of the PLLA membranes grafting a large number of free amino group on its surface which lead to the improvement of material hydrophilic,³⁹ which was beneficial for improving the material characteristics of antithrombosis.⁴³ However, the opposite charge carried by the amino and platelets did not improve the antiplatelet ideally, as shown in Figure 6(B). The results of the PT and APTT assays, as shown in Figure 7, also revealed that the clotting time of the PPP samples in the three groups had a gradual prolonged trend.

Effect of the assembled membranes to endothelial cells

The most important design objective of the SZ-21/chitosan-coated stent was to accelerate the re-endothelialization and healing process of the blood vessel wall. Therefore, the cell compatibility of this LBL coating was evaluated in an endothelial cell culture model with Eahy926 cells. As shown in Figure 8, the endothelial cells on the SZ-21/chitosan

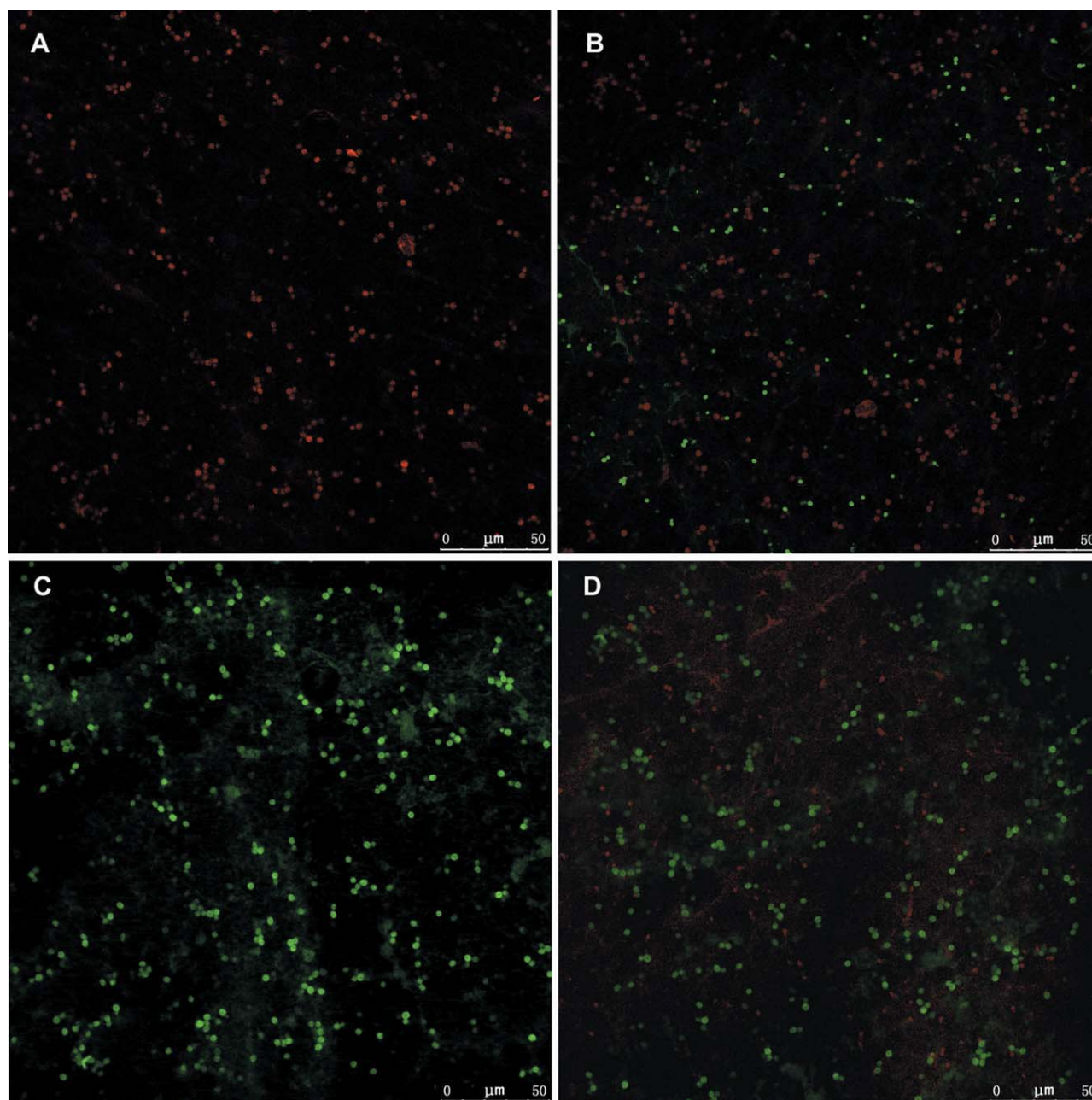


FIGURE 5. Four major distribution of SZ-21 (RBITC-labelled) and chitosan (FITC-labelled) scanned by LSCM at z-scan mode: SZ-21 monolayer (A); transition from SZ-21 monolayer to chitosan monolayer (B); chitosan monolayer (C); transition from chitosan monolayer to SZ-21 monolayer (D) [Color figure can be viewed in the online issue, which is available at wileyonlinelibrary.com].

assembled membranes formed a single layer, keeping their natural original shape. The results of endothelial cell adhesion indicated that the endothelial cells were amicable to this kind of bio-modified membrane. The free cell migration assay was used to determine the effect of the assembled coating on cell migration, for the evaluation of the activities of endothelial cells attached to the sample surfaces. As can be seen from Figure 9, the migration rates of the cells on the LBL modified samples were higher than those on the untreated PLLA membrane samples, indicating that the cells already attached to the LBL-coated surfaces retained a

strong growth and migration viability, and were much more activated, with an increase in the assembled layers.

mAb's release characteristics of the assembled stent

The other design objective of the SZ-21/chitosan-coated stent was to improve the release character of SZ-21 compared with the physically absorbed method. Our previous research³¹ had demonstrated that the SZ-21 release character of the PLLA matrix presented the standard curve of protein absorbed when released from the surface of solid matrix, which was significantly influenced by the different flow

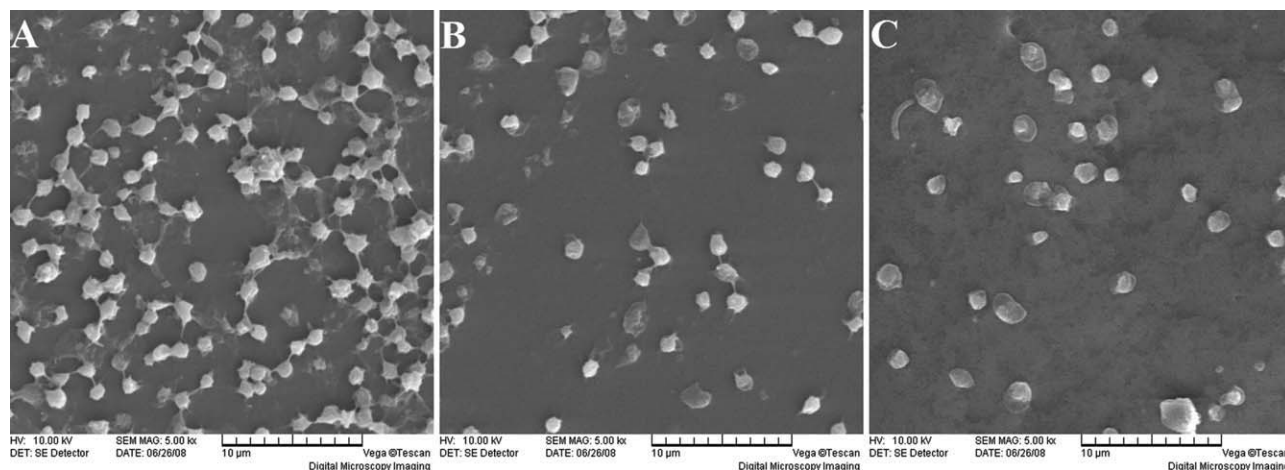


FIGURE 6. Morphology of adherent platelets on the surface of PLLA membrane (A), aminolyzed PLLA membranes (B), and assembled PLLA membranes with (SZ-21/chitosan)₁₀ layers (C) after 3 h of incubation in PRP.

rates. Therefore, in this study, the perfusion was set at the maximum rate (20 mL/min) to evaluate the release character of the different coating methods. As can be seen from Figure 10, SZ-21 could be continuously released from the different coated matrix for about 2 weeks, and 60% of the SZ-21 was still present on the SZ-21/chitosan-coated stent wires with 10 bilayers, and 50% on the SZ-21/chitosan-coated stent wires with five bilayers, but only 10% on the coated stent, when using physically absorbed method. The burst release of the SZ-21 also occurred in the three groups, but had been alleviated when using the LBL self-assembly technology to coat the stent.

DISCUSSION

The structure of the self-assembled membrane is affected by a number of factors, such as the conformation of polyelectrolyte molecules, the average charge density, and the speed of absorption, which can be controlled by adjusting the temperature, substrate, polyelectrolyte solubility, molecular chain of the charge density, solution concentration, pH value, and solvent composition. Many studies show that in a solution of considerable concentration, the strong polyelectrolyte in the solution is mainly affected by ionic strength effects, but a weak polyelectrolyte, including protein, is mainly affected by pH value and solvent polarity.⁴⁴ Most of the pH values play the most important role in the assembly process. Adjusting the pH value can significantly change the surface charge intensity, intersperse between the layers, the degree of film thickness, and so on. Thus, it is reasonable to adjust the assembly process by controlling the pH value of the assembly solution. However, during the process of the assembly, the bioactivity of the protein must be maintained in different pH buffers, so the platelet aggregation assay was used to evaluate the influence of pH on the mAb activity in present study. Platelet-platelet aggregation is an important physiological characteristic, which is an important factor in the process of hemostasis and thrombosis. Determination of platelet aggregation in thrombosis has a great significance for the clinical diagnosis of prestates and

thrombotic diseases. For a long time, detection of platelet aggregation activity has been the gold standard for *in vitro* platelet function evaluation.⁴⁵

The SZ-21 has the ability to block the GP IIb/IIIa receptors on the platelets, preventing the formation of fibrinogen bridges, the final common pathway in platelet thrombus formation.³⁰ Although the chitosan is often used as a procoagulant material, the hemostatic role of chitosan is indirect, through its nonspecific adsorption of blood cells, rather than a direct activation of the blood coagulation system.⁴⁶ From the results of APTT and PT assays, it can be suggested that SZ-21 contributed predominantly to the good anticoagulation property of the assembled multilayer membrane, as well as being an important part of the building block in this coating system.

It was reported that chitosan itself could accelerate vascular endothelial growth through inducing fibroblasts to

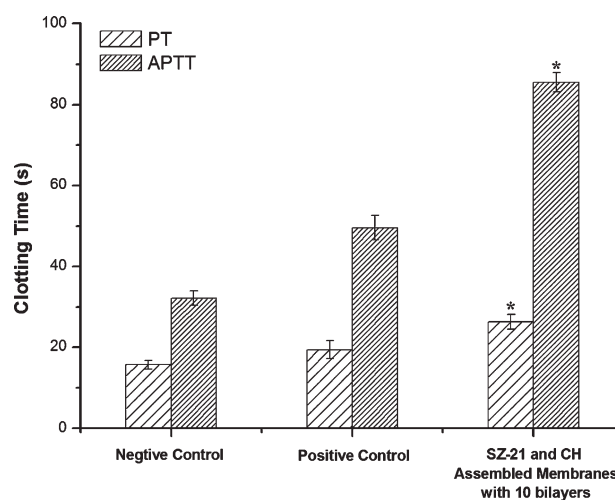


FIGURE 7. Activated partial thromboplastin time (APTT) and prothrombin time (PT) of PLLA membrane (negative control), aminolyzed PLLA membranes (positive control), and assembled PLLA membranes with (SZ-21/chitosan)₁₀ layers (C) ($n = 6$). Chitosan abbreviated as CH in this figure.

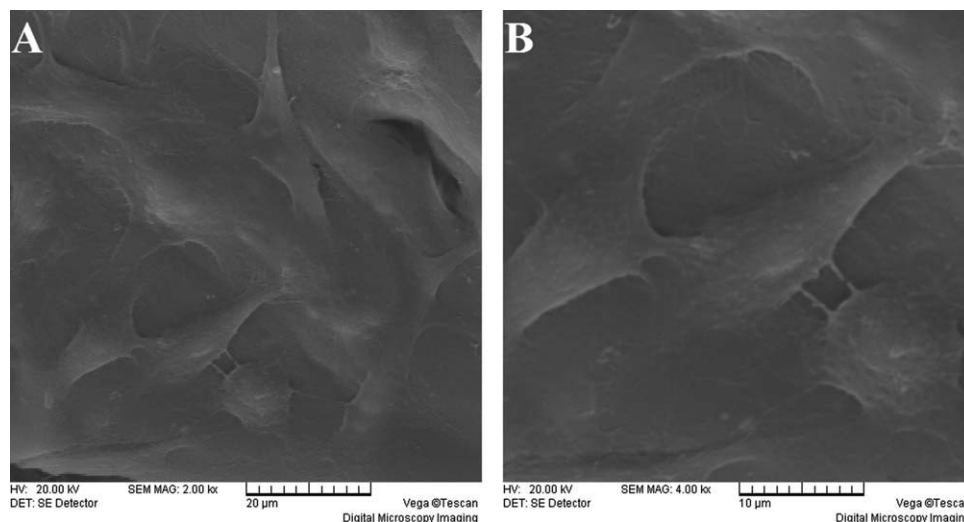


FIGURE 8. Morphology of SEM of the adherent Eahy926 cells on the assembled PLLA membranes with (SZ-21/chitosan)₁₀ layers. (A) 2000× magnification; (B) 4000× magnification.

release interleukin-8, which is involved in the migration and proliferation of fibroblasts and vascular endothelial cells.³⁴ This conclusion is further proved in this study. Although SZ-21 can inhibit vascular endothelial cell proliferation and migration through the competitive effect of the $\alpha_v\beta_3$ receptor on the membrane of endothelial cell,⁴⁷ our results about cell adhesion and migration on the SZ-21/chitosan assembled membranes prove that SZ-21 is found to contribute no negative effects to cell growth in the complex with chitosan.

The release profile has shown that the controlled release of SZ-21 by using the LBL self-assembly technology has a property of thickness dependence, which means that with the increase of assembled layers, the rate of release is more flat and slow. In the physically adsorbed stent, SZ-21 mostly permeates into the pores or defects that may exist in the polymeric matrix. However, this permeability can be under-

stood on the basis of film homogenization in the LBL technology,⁴⁸ as self-assembled films, pores or defects may exist in the films when the deposited layers are few. However, when the deposited layer thickness increase, the pores or defects can be reduced or completely closed. As a result, the film permeability decreases. Thus, the release of SZ-21 is also controlled based on this mechanism. The release of SZ-21 is also influenced by the degradation of chitosan and PLLA *in vivo*, hence, the time relationship between the release and degradation duration *in vitro* and *in vivo* must be further investigated.

CONCLUSION

These encouraging early results indicated that the monoclonal platelet GP IIIa receptor antibody SZ-21 could be used as one composition of the assembled multilayer, for its

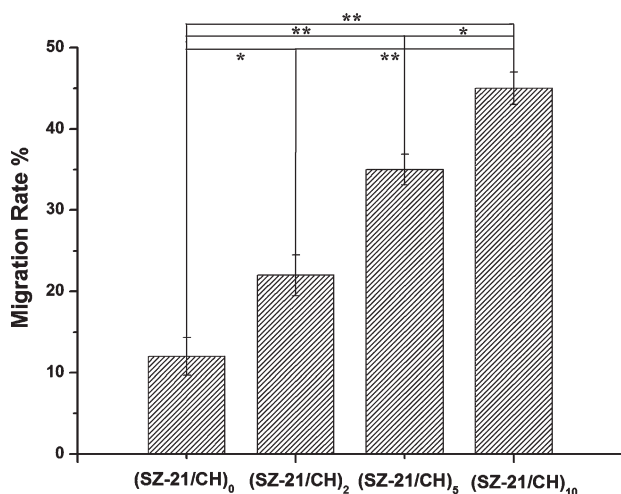


FIGURE 9. Migration rates of the cells on LBL modified samples with different layers (* $p < 0.05$, $n = 6$; ** $p < 0.01$, $n = 6$). Chitosan abbreviated as CH in this figure.

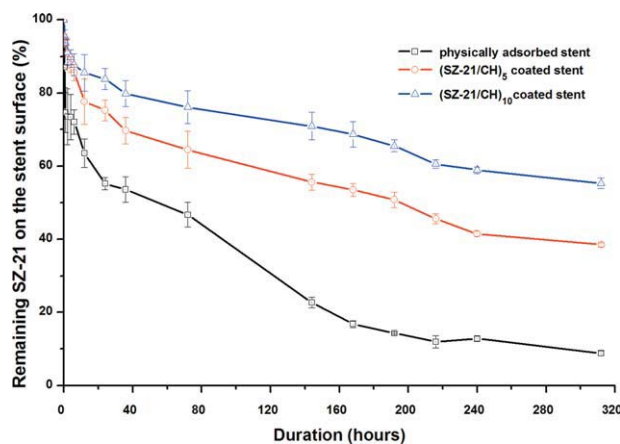


FIGURE 10. *In vitro* kinetic drug-release profiles of SZ-21 from PLLA coated stent prepared by physically adsorbed and LBL assembled method at 20 mL/min perfusion rate over 14 days in PBS-BSA at 37°C. Data are an average of three stents at each time point. Chitosan abbreviated as CH in this figure [Color figure can be viewed in the online issue, which is available at wileyonlinelibrary.com].

ability to maintain antiplatelets in different pH buffers, which demonstrated the feasibility to prepare a biocompatible stent with mAb/chitosan multilayers. The assembly process of the two kinds of materials was monitored by using fluorescence spectroscopy and confocal laser scanning microscopy scan, which proved the efficiency of the LBL assembly technology. On evaluating hemocompatibility and cytocompatibility *in vitro* when assembling the multilayer on a PLLA matrix surface, the LBL assembly method with mAb/chitosan multilayer appeared to be a promising application, to promote the antirestenosis and antithrombosis capacity of the surface-modified stent. The release of mAb from the multilayer was also evaluated by the *in vitro* perfusion system of the flow chamber, which showed an improvement in the release character compared with the passively absorbance method. Our method to prepare a biocompatible stent surface with mAb/chitosan multilayers has proved to be favorable and effective *in vitro*, thus justifying further evaluation to improve the biocompatibility in an animal model test.

REFERENCES

- Thierry B, Winnik FM, Merhi Y, Silver J, Tabrizian M. Bioactive coatings of endovascular stents based on polyelectrolyte multilayers. *Biomacromolecules* 2003;4:1564–1571.
- Hinchliffe RJ, Hopkinson BR. Development of endovascular stent-grafts. *Proc Inst Mech Eng H* 2007;221:547–560.
- Block PC, Simonton CA. STENT registry: Real-world US stent data. *J Am Coll Cardiol* 2006;48:CS1–CS6.
- Wholey MH. Current status of carotid artery stent placement. *J Cardiovasc Surg* 2006;47:101–105.
- Fischman DL, Leon MB, Baim DS, Schatz RA, Savage MP, Penn I, Detre K, Veltri L, Ricci D, Nobuyoshi M, Cleman M, Heuser R, Almond D, Teirstein PS, Fish RD, Colombo A, Brinker J, Moses J, Shakhovich A, Hirshfeld J, Bailey S, Ellis S, Rake R, Goldberg S. A randomized comparison of coronary-stent placement and balloon angioplasty in the treatment of coronary artery disease. *N Engl J Med* 1994;331:496–501.
- Serruys PW, de Jaegere P, Kiemeneij F, Macaya C, Rutsch W, Heyndrickx G, Emanuelsson H, Marco J, Legrand V, Materne P, Belardi J, Sigwart U, Colombo A, Goy JJ, Van den HP, Delcan J, Morel M. A comparison of balloon-expandable-stent implantation with balloon angioplasty in patients with coronary artery disease. *N Engl J Med* 1994;331:489–495.
- Williams DO, Holubkov R, Yeh W, Bourassa MG, Al-Bassam M, Block PC, Coady P, Cohen H, Cowley M, Dorros G, Faxon D, Holmes DR, Jacobs A, Kelsey SF, King SB 3rd, Myler R, Slater J, Stanek V, Vlachos HR, Detre KM. Percutaneous coronary intervention in the current era compared with 1985–1986: The National Heart, Lung, and Blood Institute Registries. *Circulation* 2000;102:2945–2951.
- Babapulle MN, Eisenberg MJ. Coated stents for the prevention of restenosis: Part II. *Circulation* 2002;106:2859–2866.
- Sousa JE, Serruys PW, Costa MA. New frontiers in cardiology: Drug-eluting stents: Part I. *Circulation* 2003;107:2274–2279.
- Sousa JE, Serruys PW, Costa MA. New frontiers in cardiology: drug-eluting stents: Part II. *Circulation* 2003;107:2383–2389.
- Ong AT, McFadden EP, Regar E, de Jaegere PP, van Domburg RT, Serruys PW. Late angiographic stent thrombosis (LAMB) events with drug-eluting stents. *J Am Coll Cardiol* 2005;45:2088–2092.
- Takahashi S, Kaneda H, Tanaka S, Miyashita Y, Shiono T, Takekuni Y, Domae H, Matsumi J, Mizuno S, Minami Y, Sugitatsu K, Saito S. Late angiographic stent thrombosis after sirolimus-eluting stent implantation. *Circ J* 2007;71:226–228.
- McFadden EP, Stabile E, Regar E, Cheneau E, Ong AT, Kinnaird T, Suddath WO, Weissman NJ, Torguson R, Kent KM, Pichard AD, Sattler LF, Waksman R, Serruys PW. Late thrombosis in drug-eluting coronary stents after discontinuation of antiplatelet therapy. *Lancet* 2004;364:1519–1521.
- van der Giessen WJ, Lincoff AM, Schwartz RS, van Beusekom HM, Serruys PW, Holmes DR Jr, Ellis SG, Topol EJ. Marked inflammatory sequelae to implantation of biodegradable and non-biodegradable polymers in porcine coronary arteries. *Circulation* 1996;94:1690–1697.
- Meng S, Liu ZJ, Shen L, Guo Z, Chou LSL, Zhong W, Du QG, Ge J. The effect of a layer-by-layer chitosan-heparin coating on the endothelialization and coagulation properties of a coronary stent system. *Biomaterials* 2009;30:2276–2283.
- Pendyala L, Jabara R, Robinson K, Chronos N. Passive and active polymer coatings for intracoronary stents: Novel devices to promote arterial healing. *J Interv Cardiol* 2009;22:37–48.
- Schwartz RS, Chronos NA, Virmani R. Preclinical restenosis models and drug-eluting stents: Still important, still much to learn. *J Am Coll Cardiol* 2004;44:1373–1385.
- Finn AV, Nakazawa G, Joner M, Kolodgie FD, Mont EK, Gold HK, Virmani R. Vascular responses to drug eluting stents: Importance of delayed healing. *Arterioscler Thromb Vasc Biol* 2007;27:1500–1510.
- Hardhammar PA, van Beusekom HM, Emanuelsson HU, Hofma SH, Albertsson PA, Verdouw PD, Boersma E, Serruys PW, van der Giessen WJ. Reduction in thrombotic events with heparin-coated Palmaz-Schatz stents in normal porcine coronary arteries. *Circulation* 1996;93:423–430.
- Whelan DM, van der Giessen WJ, Krabbendam SC, van Vliet EA, Verdouw PD, Serruys PW, van Beusekom HM. Biocompatibility of phosphorylcholine coated stents in normal porcine coronary arteries. *Heart* 2000;83:338–345.
- Holmes DR, Camrud AR, Jorgenson MA, Edwards WD, Schwartz RS. Polymeric stenting in the porcine coronary artery model: Differential outcome of exogenous fibrin sleeves versus polyurethane-coated stents. *J Am Coll Cardiol* 1994;24:525–531.
- Park K, Shim HS, Dewanjee MK, Eigler NL. In vitro and in vivo studies of PEO-grafted blood-contacting cardiovascular prostheses. *J Biomater Sci Polym Ed* 2000;11:1121–1134.
- Aggarwal RK, Ireland DC, Azrin MA, Ezekowitz MD, de Bono DP, Gershlick AH. Antithrombotic potential of polymer-coated stents eluting platelet glycoprotein IIb/IIIa receptor antibody. *Circulation* 1996;94:3311–3317.
- Baron JH, Gershlick AH, Hogrefe K, Armstrong J, Holt CM, Aggarwal RK, Azrin M, Ezekowitz M, de Bono DP. In vitro evaluation of c7E3-Fab (ReoPro) eluting polymer-coated coronary stents. *Cardiovasc Res* 2000;46:585–594.
- Aoki J, Serruys PW, van Beusekom H, Ong AT, McFadden EP, Sianos G, van der Giessen WJ, Regar E, de Feyter PJ, Davis HR, Rowland S, Kutryk MJ. Endothelial progenitor cell capture by stents coated with antibody against CD34: the HEALING-FIM (Healthy Endothelial Accelerated Lining Inhibits Neointimal Growth-First In Man) Registry. *J Am Coll Cardiol* 2005;45:1574–1579.
- Waksman R. Drug-eluting stents: From bench to bed. *Cardiovasc Radiat Med* 2002;3:226–241.
- Nakayama Y, Nishi S, Ishibashi-Ueda H. Fabrication of drug-eluting covered stents with micropores and differential coating of heparin and FK506. *Cardiovasc Radiat Med* 2003;4:77–82.
- Verhoeven ML, Driessen AA, Paul AJ, Brown A, Canry JC, Hendriks M. DSIMS characterization of a drug-containing polymer-coated cardiovascular stent. *J Control Release* 2004;96:113–121.
- Hammond PT. Form and function in multilayer assembly: New applications at the nanoscale. *Adv Mater* 2004;16:1271–1293.
- Yin T, Wang G, Ruan C, Guzman R, Guidoin R. In-vitro assays of polymer-coated stents eluting platelet glycoprotein IIb/IIIa receptor monoclonal antibody. *J Biomed Mater Res A* 2007;83:861–867.
- Wang GX, Luo LL, Yin TY, Li Y, Jiang T, Ruan CG, Guidoin R, Chen YP, Guzman R. Ultrasonic atomization and subsequent desolvation for monoclonal antibody (mAb) to the glycoprotein (GP) IIIa receptor into drug eluting stent. *J Microencapsul* 2010;27:105–114.
- An G, Dong N, Shao B, Zhu M, Ruan C. Preparation and characterization of a single chain antibody fragment of mAb SZ-21 against platelets GPIIa. *Zhonghua Xue Ye Xue Za Zhi* 2002;23:480–482.
- Macdonald M, Rodriguez NM, Smith R, Hammond PT. Release of a model protein from biodegradable self assembled films for surface delivery applications. *J Control Release* 2008;131:228–234.

34. Zhu Y, Gao C, Liu X, He T, Shen J. Immobilization of biomacromolecules onto aminolyzed poly(L-lactic acid) toward acceleration of endothelium regeneration. *Tissue Eng* 2004;10:53–61.
35. Zhu A, Zhao F, Ma T. Photo-initiated grafting of gelatin/N-maleic acyl-chitosan to enhance endothelial cell adhesion, proliferation and function on PLA surface. *Acta Biomater* 2009;5:2033–2044.
36. Thierry B, Merhi Y, Silver J, Tabrizian M. Biodegradable membrane-covered stent from chitosan-based polymers. *J Biomed Mater Res A* 2005;75:556–566.
37. Sarisozen C, Arica B, Hincal AA, Calis S. Development of biodegradable drug releasing polymeric cardiovascular stents and in vitro evaluation. *J Microencapsul* 2009;26:501–512.
38. Born GVR. Aggregation of blood platelets by adenosine diphosphate and its reversal. *Nature* 1962;194:927.
39. Zhu YB, Gao CY, He T, Liu XY, Shen JC. Layer-by-layer assembly to modify poly(L-lactic acid) surface toward improving its cytocompatibility to human endothelial cells. *Biomacromolecules* 2003;4:446–452.
40. Jiang T, Wang G, Qiu J, Luo L, Zhang G. Heparinized poly(vinyl alcohol)-small intestinal submucosa composite membrane for coronary covered stents. *Biomed Mater* 2009;4:025012.
41. Luo LL, Wang GX, Yin TY, Shen Y, Hou YB, Li Y, Jiang T. A novel micro-spraying system for preparing polymer-coated intravascular stent. Proceedings of the IEEE/ICME International Conference on Complex Med Eng, Beijing, May 23–27, 2007. p 1956–1960.
42. Schlenoff JB, Dubas ST. Mechanism of polyelectrolyte multilayer growth: charge overcompensation and distribution. *Macromolecules* 2001;34:592–598.
43. Seeger JM, Ingegno MD, Bigatan E, Klingman N, Amery D, Widenhouse C, Goldberg EP. Hydrophilic surface modification of metallic endoluminal stents. *J Vasc Surg* 1995;22:327–336.
44. Choi J, Rubner MF. Influence of the degree of ionization on weak polyelectrolyte multilayer assembly. *Macromolecules* 2005;38:116–124.
45. Moran N, Kiernan A, Dunne E, Edwards RJ, Shields DC, Kenny D. Monitoring modulators of platelet aggregation in a microtiter plate assay. *Anal Biochem* 2006;357:77–84.
46. Klokkevold PR, Subar P, Fukayama H, Bertolami CN. Effect of chitosan on lingual hemostasis in rabbits with platelet dysfunction induced by epoprostenol. *J Oral Maxillofac Surg* 1992;50:41–45.
47. Choi ET, Engel L, Callow AD, Sun S, Trachtenberg J, Santoro S, Ryan US. Inhibition of neointimal hyperplasia by blocking alpha V beta 3 integrin with a small peptide antagonist GpenGRGDSPCA. *J Vasc Surg* 1994;19:125–134.
48. Qiu XP, Donath E, Mohwald H. Permeability of ibuprofen in various polyelectrolyte multilayers. *Macromol Mater Eng* 2001;286:591–597.